Supplementary Material

A Unified Framework for Psychometrics in Experimental Psychology: The Standardized Generalized Hierarchical Factor Model

Ricardo Rey-Sáez[1], Alicia Franco-Martínez[1], Javier Revuelta[2], and Miguel A. Vadillo[1]

[1]Department of Basic Psychology, Universidad Autónoma de Madrid

[2]Department of Social Psychology and Methodology, Universidad Autónoma de Madrid

Author Note

Ricardo Rey-Sáez https://orcid.org/0000-0001-6739-2035

Alicia Franco-Martínez https://orcid.org/0000-0002-9710-1240

Javier Revuelta https://orcid.org/0000-0003-4705-6282

Miguel A. Vadillo https://orcid.org/0000-0001-8421-816X

All data, models, and sripts required to reproduce the results of this work are publicly available at https://osf.io/5dutv/ and https://github.com/RicardoReySaez/GenHFM.

Correspondence concerning this article should be addressed to Ricardo Rey-Sáez, Department of Basic Psychology, Universidad Autónoma de Madrid, Ivan Pavlov Street, 6, Fuencarral-El Pardo, Madrid 28049, Spain, Email: ricardoreysaez95@gmail.com

SM1: Equivalence between Spearman correction for attenuation and frequentist hierarchical models

Previous work has suggested that hierarchical models provide more precise estimates of correlations between experimental effects than the traditional Spearman correction for attenuation (Mehrvarz & Rouder, 2025; Rouder et al., 2023). We show, however, that this apparent gain in precision is not due to the hierarchical structure per se, but rather to the use of Bayesian estimation, where prior distributions act as regularizers. Both Rouder et al. (2023) and Mehrvarz and Rouder (2025) model these matrices using an inverse-Wishart prior,

$$\mathbf{\Sigma}_\beta \sim \text{Inverse-Wishart}\left(\nu = J + 1,\ \mathbf{\Psi} = a^2 \cdot \mathbf{I}\right)$$

where ν and $\mathbf{\Psi}$ are the shape and scale parameters of the inverse Wishart distribution, J is the number of tasks, $\mathbf{I}$ is a $J \times J$ identity matrix and a^2 is desCIbed by the authors as "a prior setting that corresponds to the prior expected value of variance" (Mehrvarz & Rouder, 2025, p. 4). In their simulation study, the authors set $a^2 = 0.025^2$ as the prior variance parameter while generating the data using the same population variance value, $\sigma_\beta^2 = 0.025^2$. Consequently, the prior is intended to be centered on the true value used to generate the data in their simulation studies.

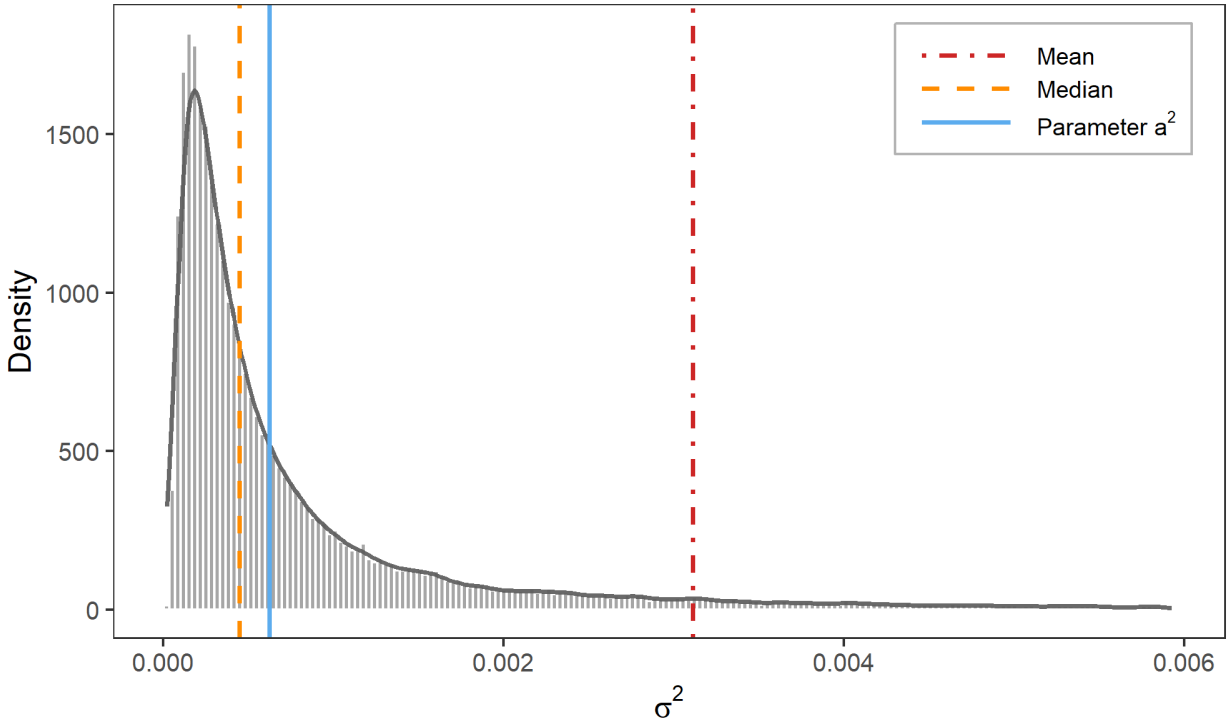
However, it is worth noting that a^2 does not correspond strictly to the expected value of the variance in this setting. For an inverse-Wishart prior in J dimensions, the mean $\mathbb{E}[\mathbf{\Sigma}]$ exists only if $\nu > J + 1$, and the element-wise variances exist only if $\nu > J + 3$. With the choice $\nu = J + 1$, neither the mean nor the variance are finite. Therefore, a^2 functions as a scale parameter, but its interpretation as a "prior expected variance" is technically imprecise given the selected degrees of freedom.

To better illustrate the influence of the parameter a, we simulated 50,000 samples from the inverse-Wishart distribution with $J = 2$ and $a^2 = 0.025^2$, and examined the resulting marginal distribution of the variance components (Figure S1). As shown, this prior assigns a large proportion of its probability mass to values very close to zero, while remaining extremely diffuse

for larger variances. Approximately 61% of the simulated values fall below a^2, whereas the remaining 39% are spread between 0.025^2 and infinity. Overall, this prior tends to regularize variance estimates toward zero.

Figure S1

Sampling distribution of variance values drawn from the inverse-Wishart prior



Although this inverse-Wishart prior is uniform over the space of correlations, its regularization on the variances affects the posterior distribution of the correlations. To illustrate this point, we replicated the simulation reported by Rouder et al. (2023) for estimating the correlation between two tasks, using their original `R` code. The only modification we introduced was to vary the true population correlation between tasks from .1 to .9 in increments of .1. For each value of the true correlation, we simulated 1,000 datasets and estimated the correlation using three methods: the Spearman correction for attenuation, a frequentist hierarchical model, and the Bayesian hierarchical model implementing the exact inverse-Wishart prior parametrization used by Rouder et al. (2023) and Mehrvarz and Rouder (2025). Given that the frequentist hierarchical model relies solely on the likelihood without incorporating prior distributions, this comparison

serves to isolate the shrinkage effect introduced specifically by the inverse-Wishart prior.

Figure S2

Sampling distribution of correlation estimates with the Spearman correction for attenuation, frequentist and Bayesian hierarchical model (HM)

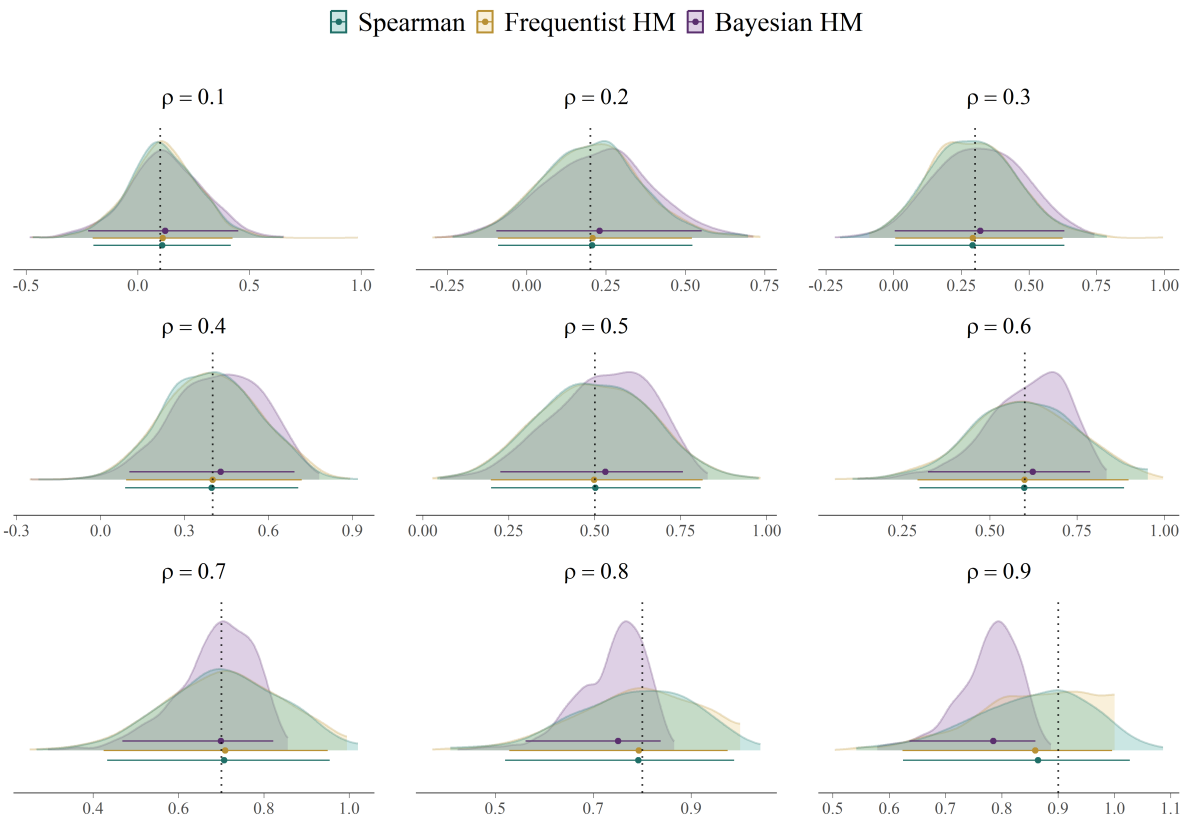


Figure S2 shows the sampling distributions of the 1,000 correlation estimates obtained with each method (posterior means for the Bayesian model). Across all values of the true correlation, Spearman's correction for attenuation and the frequentist hierarchical model yield nearly identical estimates. In contrast, the Bayesian hierarchical model appears increasingly precise as the true correlation grows. Table S1 summarizes the standard deviations of these sampling distributions: while Spearman's correction and the frequentist model produce almost identical variability, the Bayesian model shows larger dispersion when ρ is low and smaller dispersion when ρ is high. However, at high true correlations ($\rho = .8$ and $\rho = .9$), this apparent gain in precision reflects overconfidence rather than accuracy, and the posterior means become

systematically biased away from the true value. Only around $\rho = .3$ or $\rho = .4$ do the three methods display comparable uncertainty and accuracy.

Table S1

Sampling standard deviation of the distribution of correlation estimates with Spearman method and both frequentist and Bayesian HM (Hierarchical Models)

Method	$\rho = 0.1$	$\rho = 0.2$	$\rho = 0.3$	$\rho = 0.4$	$\rho = 0.5$	$\rho = 0.6$	$\rho = 0.7$	$\rho = 0.8$	$\rho = 0.9$
Spearman	0.155	0.155	0.158	0.164	0.158	0.154	0.141	0.121	0.098
Frequentist HM	0.159	0.158	0.166	0.166	0.160	0.154	0.140	0.119	0.097
Bayesian HM	0.171	0.166	0.165	0.162	0.143	0.125	0.097	0.074	0.054

Overall, the practical equivalence between Spearman's correction and the frequentist hierarchical model, together with their divergence from the Bayesian hierarchical model, indicates that the added precision is a consequence of the prior specification, not of the hierarchical structure itself.

SM2: Expected Values and Variances of Zero-Truncated Normal Distributions

To ensure positive values, the parameters σ and τ were modeled as zero-truncated normal distributions. Let $\alpha = (a - \mu_X)/\sigma_X$, with $a = 0$ denoting the lower truncation limit. For a truncated normal variable X, the expected value and variance are (Greene, 2011, p. 836):

$$\mathbb{E}[X] = \mu_X + \sigma_X \cdot \lambda(\alpha) \quad \text{and} \quad \mathbb{V}[X] = \sigma^2 \cdot [1 - \delta(\alpha)] \tag{1}$$

where μ_X and σ_X^2 denote the mean and variance of the untruncated normal distribution, respectively, and

$$\lambda(\alpha) = \frac{\phi(\alpha)}{1 - \Phi(\alpha)}, \qquad \delta(\alpha) = \lambda(\alpha) \cdot [\lambda(\alpha) - \alpha], \tag{2}$$

with $\phi(\cdot)$ and $\Phi(\cdot)$ being the standard normal probability density and cumulative distribution functions, respectively.

To optimize sampling in *Stan*, we adopted a two-step procedure to define the truncated distribution. First, the variable Z was defined as a standardized normal variable truncated at zero. In this case, $\mu_Z = 0$ and $\sigma_Z = 1$, $\alpha = 0/1 = 0$, so the standardized truncation point is $\alpha = (0 - 0)/1 = 0$. Consequently,

$$\lambda(0) = \frac{\phi(0)}{1 - \Phi(0)}, \tag{3}$$

where $\phi(0)$ and $\Phi(0)$ denote the standard normal density and cumulative distribution evaluated at zero whose values are $1/\sqrt{2 \cdot \pi}$ and $1/2$, respectively. Substituting these values yields $\lambda(0) = \sqrt{2/\pi}$, and therefore the expected value and variance of the standardized truncated normal distribution are

$$\mathbb{E}[Z] = \sqrt{\frac{2}{\pi}} \quad \text{and} \quad \mathbb{V}[Z] = 1 - \frac{2}{\pi}. \tag{4}$$

Next, we defined the variable $Y = \text{shift} + \text{scale} \cdot Z$ where *shift* and *scale* are positive-valued parameters. The expected value and variance of Y can then be obtained by a change of variable:

$$\mathbb{E}[Y] = \text{shift} + \text{scale} \cdot \mathbb{E}[Z], \qquad \mathbb{V}[Y] = \text{scale}^2 \cdot \mathbb{V}[Z] \tag{5}$$

The main limitation of this approximation is that it does not provide direct access to the mean and variance of the corresponding untruncated normal distribution. To recover these quantities, it is necessary to establish the equivalence between *shift* and *scale* and the parameters μ_X and σ_X^2 of the untruncated distribution.

From μ_X and σ_X to *shift* and *scale*

Starting from known values of μ_X and σ_X, *shift* and *scale* can be obtained analytically. First, by equating the variances of Y and X and solving for *scale*:

$$\begin{aligned}
\mathbb{V}[Y] &= \mathbb{V}[X] \\
\text{scale}^2 \cdot \mathbb{V}[Z] &= \sigma_X^2 \cdot [1 - \delta(\alpha)] \\
\text{scale}^2 \cdot \left[1 - \frac{2}{\pi}\right] &= \sigma_X^2 \cdot [1 - \delta(\alpha)] \\
\text{scale}^2 &= \frac{\sigma_X^2 \cdot [1 - \delta(\alpha)]}{\left[1 - \frac{2}{\pi}\right]} \\
\text{scale} &= \sigma_X \cdot \sqrt{\frac{1 - \delta(\alpha)}{\left[1 - \frac{2}{\pi}\right]}}
\end{aligned} \tag{6}$$

Once *scale* is known, *shift* can be obtained from the equality of expected values:

$$\begin{aligned}
\mathbb{E}[Y] &= \mathbb{E}[X] \\
\text{shift} + \text{scale} \cdot \mathbb{E}[Z] &= \mu_X + \sigma_X \cdot \lambda(\alpha) \\
\text{shift} + \text{scale} \cdot \sqrt{\frac{2}{\pi}} &= \mu_X + \sigma_X \cdot \lambda(\alpha) \\
\text{shift} &= \mu_X + \sigma_X \cdot \lambda(\alpha) - \text{scale} \cdot \sqrt{\frac{2}{\pi}}
\end{aligned} \tag{7}$$

Although these expressions allow computing *shift* and *scale* given μ_X and σ_X, the inverse transformation (i.e., recovering μ_X and σ_X from *shift* and *scale*) has no closed-form solution and must be solved numerically. This is because the parameters are linked through the standardized

truncation point, α, which simultaneously depends on both μ_X and σ_X. Moreover, the functions $\lambda(\alpha)$ and $\delta(\alpha)$ involve the standard normal cumulative distribution, $\Phi(\alpha)$, whose inverse has no analytic expression.

From *shift* and *scale* to μ_X and σ_X

We reparameterized the truncated normal formulation in terms of α and σ_X. Since $\alpha = (a - \mu_X)/\sigma_X$ and $a = 0$, it follows that $\mu_X = -\alpha \cdot \sigma_X$. Using Equation 6, we can solve for σ_X^2:

$$\begin{aligned} \text{scale}^2 &= \frac{\sigma_X^2 \cdot [1 - \delta(\alpha)]}{\left[1 - \frac{2}{\pi}\right]} \\ \frac{\text{scale}^2 \cdot \left[1 - \frac{2}{\pi}\right]}{1 - \delta(\alpha)} &= \sigma_X^2 \end{aligned} \tag{8}$$

Next, from Equation 7, we can solve for σ_X:

$$\begin{aligned} \text{shift} + \text{scale} \cdot \sqrt{\frac{2}{\pi}} &= \mu_X + \sigma_X \cdot \lambda(\alpha) \\ \text{shift} + \text{scale} \cdot \sqrt{\frac{2}{\pi}} &= -\alpha \cdot \sigma_X + \sigma_X \cdot \lambda(\alpha) \\ \text{shift} + \text{scale} \cdot \sqrt{\frac{2}{\pi}} &= \sigma_X \cdot [\lambda(\alpha) - \alpha] \\ \frac{\text{shift} + \text{scale} \cdot \sqrt{\frac{2}{\pi}}}{\lambda(\alpha) - \alpha} &= \sigma_X \end{aligned} \tag{9}$$

We can now square Equation 9 and set it equal to Equation 8, leaving α as the only unknown parameter:

$$\left(\frac{\text{shift} + \text{scale} \cdot \sqrt{\frac{2}{\pi}}}{\lambda(\alpha) - \alpha} \right)^2 = \frac{\text{scale}^2 \cdot \left[1 - \frac{2}{\pi}\right]}{1 - \delta(\alpha)} \tag{10}$$

Rearranging, we define the target function $f(\alpha)$:

$$f(\alpha) = \left(\frac{\text{shift} + \text{scale} \cdot \sqrt{\frac{2}{\pi}}}{\lambda(\alpha) - \alpha} \right)^2 - \frac{\text{scale}^2 \cdot \left[1 - \frac{2}{\pi}\right]}{1 - \delta(\alpha)} = 0 \tag{11}$$

The goal is to identify the value of α that satisfies $f(\alpha) = 0$, which can be done numerically using standard root-finding or standard optimization methods. Once α is estimated, σ_X^2 can be obtained from either Equation 8 or Equation 9, and μ_X follows directly as $\mu_X = -\alpha \cdot \sigma_X$. The R code below implements the function $f(\alpha)$ using a least-squares approach. For demonstration, the example sets shift = 0.2 and scale = 0.3, although in practice these would be replaced by the values of interest.

```r
# Shift and scale fixed values
shift <- .2; scale <- .3

# Lambda and delta functions
lambda <- function(alpha) dnorm(alpha) / (1 - pnorm(alpha))
delta  <- function(alpha) lambda(alpha) * (lambda(alpha) - alpha)

# Least-squares objective f(alpha) function
f_alpha <- function(alpha, shift, scale){
  # Variance from Eq. (9)
  S2X_eq1 <- ((shift + scale * sqrt(2/pi)) / (lambda(alpha) - alpha))^2
  # Variance from Eq. (8)
  S2X_eq2 <- (scale^2 * (1 - 2/pi)) / (1 - delta(alpha))
  # Squared difference between variance estimates
  (S2X_eq1 - S2X_eq2)^2
}

# Minimize f(alpha) function to estimate alpha
fit_LS <- optim(par = 0, fn = f_alpha, shift = shift, scale = scale,
                method = "BFGS")

# Store the estimated alpha value that minimizes the squared differences
alpha_LS <- fit_LS$par

# Recover mu and sigma parameters from alpha
sigma_LS <- (shift + scale * sqrt(2/pi)) / (lambda(alpha_LS) - alpha_LS)
mu_LS <- -alpha_LS * sigma_LS
```

SM3: Expected Values for σ^2 and τ^2

As noted in the main text, reliability calculations depend on μ_{σ^2} for the shifted-lognormal model and on μ_{σ^2} and μ_{τ^2} for the ex-Gaussian model. Here, to maintain consistency with the notation introduced in the previous subsection, we denote these quantities as $\mathbb{E}\left[\sigma^2\right]$ and $\mathbb{E}\left[\tau^2\right]$. These expectations, however, are not directly available and cannot be computed simply as $(\mathbb{E}[\sigma])^2$ or $(\mathbb{E}[\tau])^2$. The key point is that the square of the mean is not equivalent to the mean of the squared quantities. In other words, squaring the average of the standard deviation parameters is not the same as averaging the squared values of these standard deviations (i.e., the mean of a distribution of variances).

This distinction arises because the squaring function ($x \mapsto x^2$) is convex, and according to Jensen's inequality, $\mathbb{E}\left[x^2\right] \geq (\mathbb{E}\left[x\right])^2$. As a result, using squared means would systematically underestimate the true expected variances $\mathbb{E}\left[\sigma^2\right]$ and $\mathbb{E}\left[\tau^2\right]$. When applied to reliability calculations, this underestimation of variance leads to inflated reliability estimates.

This quadratic expectation can be obtained directly from the basic definition of the variance of a random variable, $\mathbb{V}\left[X\right] = \mathbb{E}[X^2] - (\mathbb{E}[X])^2$, so that $\mathbb{E}[X^2]$ can be expressed as $\mathbb{E}[X^2] = (\mathbb{E}[X])^2 + \mathbb{V}\left[X\right]$.

We simply apply this relation to derive the expected quadratic terms $\mathbb{E}[\sigma^2]$ and $\mathbb{E}[\tau^2]$ from the means and variances of their corresponding truncated normal distributions. Substituting the expressions from Equation 5 for $\mathbb{E}[X]$ and $\mathbb{V}[X]$, the expected square becomes

$$\begin{aligned} \mathbb{E}[X^2] &= (\text{shift} + \text{scale} \cdot \mathbb{E}\left[Z\right])^2 + \text{scale}^2 \cdot \mathbb{V}\left[Z\right] \\ &= \left(\text{shift} + \text{scale} \cdot \sqrt{\frac{2}{\pi}}\right)^2 + \text{scale}^2 \cdot \left[1 - \frac{2}{\pi}\right] \end{aligned} \tag{12}$$

This expression provides a closed-form solution for $\mathbb{E}[X^2]$ in terms of the *shift* and *scale* parameters of the truncated normal distribution, which can then be directly used to compute $\mathbb{E}[\sigma^2]$ and $\mathbb{E}[\tau^2]$ for the shifted-lognormal and ex-Gaussian models, respectively.

However, no closed-form solution exists for the expected value $\mathbb{E}\left[1/\text{rate}^2\right]$ in the

ex-Gaussian model parameterized with the exponential rate parameter. To compute reliability, we can approximate $\mathbb{E}[\tau^2]$ using an inner Monte Carlo step. For each task j and posterior draw s, the expectation $\mathbb{E}[\tau^2]$ can be approximated as

$$\mathbb{E}[\tau_j^2]^{(s)} = \frac{1}{B} \sum_{b=1}^{B} \frac{1}{\left(\text{shift}_j^{(s)} + \text{scale}_j^{(s)} \cdot Z_b\right)^2}, \qquad Z_b \sim \text{Normal}^+(0, 1)\,, \tag{13}$$

that is, the average of $1/rate^2$ evaluated at B samples from the truncated standard normal distribution.

SM4: Rotational indeterminancy and identification

In exploratory factor models, the population covariance matrix is defined as $\mathbf{\Sigma} = \mathbf{\Lambda} \cdot \mathbf{\Lambda}' + \mathbf{\Psi}$. A CItical consequence of this definition is that the likelihood is evaluated in terms of $\mathbf{\Sigma}$, not the particular configuration of factor loadings $\mathbf{\Lambda}$ that produces it. Therefore, infinitely many combinations of $\mathbf{\Lambda}$ (via rotation, column permutation, or sign flipping) can yield the exact same covariance matrix.

In Bayesian estimation, this indeterminacy implies that the likelihood surface is multimodal. The MCMC sampler explores these equally valid but differently rotated solutions, exhibiting random sign flips and changing factor orders across iterations. Consequently, standard posterior summaries are meaningless; for example, averaging loadings across unaligned draws causes the means to converge to zero due to symmetry.

To address this, we avoided imposing hard constraints during estimation (e.g., fixing zeros), which can bias the factor structure (Anderson & Rubin, 1956; Carvalho et al., 2008; Papastamoulis & Ntzoufras, 2022). Instead, we employed a *post hoc* strategy using the *MatchAlign* algorithm (Poworoznek et al., 2024). This method allows the sampler to explore the posterior freely and aligns the samples after estimation in three steps: (1) Each posterior draw is orthogonally rotated (using Varimax) to anchor the orientation; (2) a representative draw (pivot) is selected based on the median leading (largest) eigenvalue; finally, (3) all other draws are aligned to the pivot via signed permutations to resolve label switching and sign ambiguity.

For unidimensional and confirmatory models, rotational indeterminacy is resolved by design (due to the single column or fixed zero constraints). However, sign indeterminacy remains. To resolve this, we followed the strategy implemented in `{blavaan}` (Merkle et al., 2021): after estimation, we constrained one anchor loading per factor to be strictly positive, flipping the signs of the corresponding factor column (and associated correlations) in any draw where the anchor was negative.

SM5: Scaled-Beta probability density function

Let $X \sim \text{Beta}\,(\alpha,\ \beta)$ defined on the interval (0,1). The probability density function of X is

$$f_X(x) = \frac{1}{\text{B}(\alpha,\beta)}\, x^{\alpha-1} \cdot (1-x)^{\beta-1}, \qquad \alpha > 0,\ \beta > 0,$$

where $\text{B}(\alpha,\beta)$ is the Beta function,

$$\text{B}(\alpha,\beta) = \frac{\Gamma(\alpha)\cdot\Gamma(\beta)}{\Gamma(\alpha+\beta)}.$$

We can re-scale this distribution to the interval (-1,1) applying the transformation $Y = 2 \cdot X - 1$. The Jacobian of this transformation is $\left|\frac{dX}{dY}\right| = \frac{1}{2}$. By change of variables, the density of Y becomes

$$\begin{aligned} f_Y(y) &= f_X\left(\tfrac{y+1}{2}\right) \cdot \left|\tfrac{dX}{dY}\right| \\ &= \frac{1}{\text{B}(\alpha,\beta)} \cdot \left(\frac{y+1}{2}\right)^{\alpha-1} \cdot \left(1-\frac{y+1}{2}\right)^{\beta-1} \cdot \frac{1}{2} \\ &= \frac{2^{-(\alpha+\beta-1)}}{\text{B}(\alpha,\beta)} \cdot (1+y)^{\alpha-1} \cdot (1-y)^{\beta-1}, \qquad y \in (-1,1), \end{aligned}$$

and the log-density is given by:

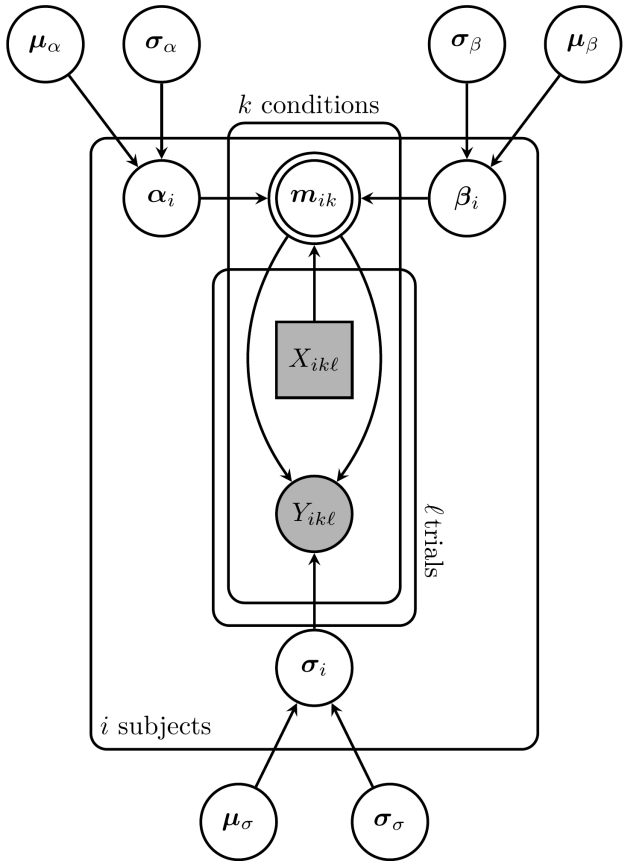
$$\log f_Y(y) = (\alpha-1)\cdot\log(1+y) + (\beta-1)\cdot\log(1-y) -$$

$$(\alpha+\beta-1)\cdot\log(2) - \log \text{B}(\alpha,\beta)$$

SM6: Bayesian hierarchical model specifications

Gaussian hierarchial model

Figure S3
Gaussian hierarchical model diagram

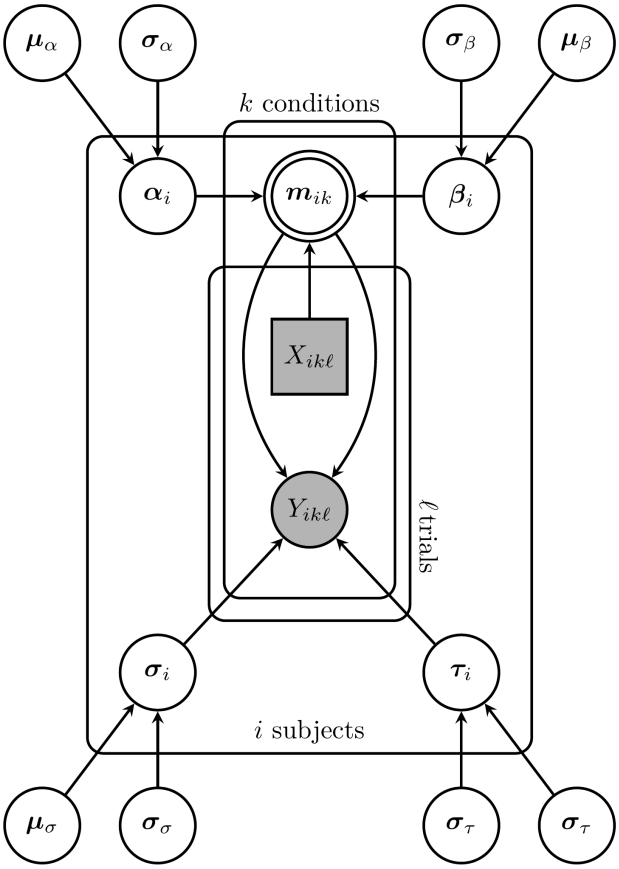


$$
\begin{aligned}
\mu_\alpha &\sim \text{Normal}^+\,(\mu = 0,\, \sigma = 10) \\
\mu_\beta &\sim \text{Normal}\,(\mu = 0,\, \sigma = 10) \\
\mu_\sigma &\sim \text{Normal}^+\,(\mu = 0,\, \sigma = 10) \\
\sigma_\alpha &\sim \text{Inverse-Gamma}\,(\alpha = 0.5,\, \beta = 0.5) \\
\sigma_\beta &\sim \text{Inverse-Gamma}\,(\alpha = 0.5,\, \beta = 0.5) \\
\sigma_\sigma &\sim \text{Inverse-Gamma}\,(\alpha = 0.5,\, \beta = 0.5) \\
\boldsymbol{\alpha}_i &\sim \text{Normal}\,(\mu = \mu_\alpha,\, \sigma = \sigma_\alpha) \\
\boldsymbol{\beta}_i &\sim \text{Normal}\,(\mu = \mu_\beta,\, \sigma = \sigma_\beta) \\
\boldsymbol{\sigma}_i &\sim \text{Normal}^+\,(\mu = \mu_\sigma,\, \sigma = \sigma_\sigma) \\
\boldsymbol{m}_{ik} &= \begin{cases} \boldsymbol{\alpha}_i - \frac{1}{2} \cdot \boldsymbol{\beta}_i & \text{if } X_{ik\ell} = 1 \\ \boldsymbol{\alpha}_i + \frac{1}{2} \cdot \boldsymbol{\beta}_i & \text{if } X_{ik\ell} = 2 \end{cases} \\
Y_{ik\ell} &\sim \text{Normal}\,(\mu = \boldsymbol{m}_{ik},\, \sigma = \boldsymbol{\sigma}_i)
\end{aligned}
$$

Ex-Gaussian hierarchial model (τ parameterization)

Figure S4

Ex-Gaussian hierarchical model diagram: τ parameterization

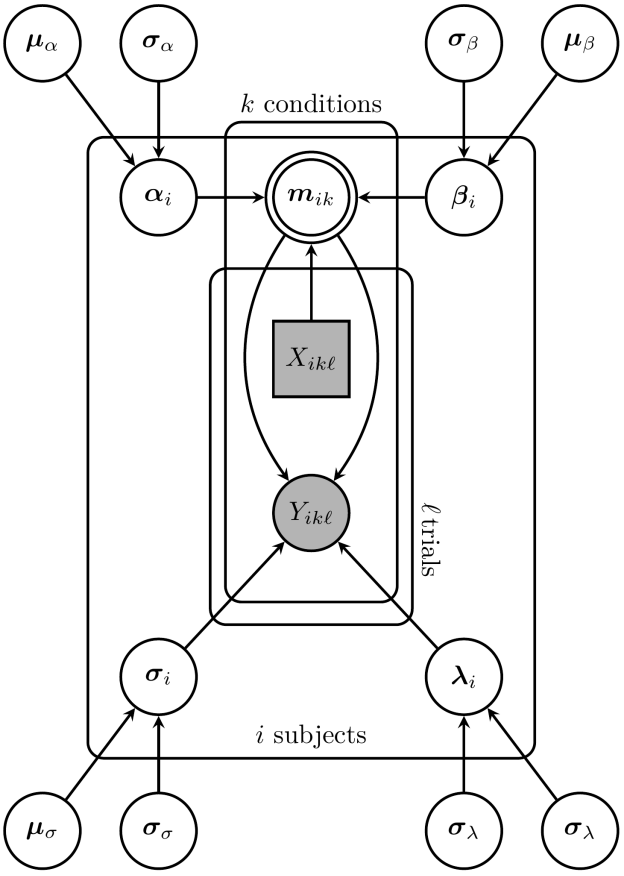


$$
\begin{aligned}
\mu_\alpha &\sim \text{Normal}^+\,(\mu = 0,\, \sigma = 10) \\
\mu_\beta &\sim \text{Normal}\,(\mu = 0,\, \sigma = 10) \\
\mu_\sigma &\sim \text{Normal}^+\,(\mu = 0,\, \sigma = 10) \\
\mu_\tau &\sim \text{Normal}^+\,(\mu = 0,\, \sigma = 10) \\
\sigma_\alpha &\sim \text{Inverse-Gamma}\,(\alpha = 0.5,\, \beta = 0.5) \\
\sigma_\beta &\sim \text{Inverse-Gamma}\,(\alpha = 0.5,\, \beta = 0.5) \\
\sigma_\sigma &\sim \text{Inverse-Gamma}\,(\alpha = 0.5,\, \beta = 0.5) \\
\sigma_\tau &\sim \text{Inverse-Gamma}\,(\alpha = 0.5,\, \beta = 0.5) \\
\boldsymbol{\alpha}_i &\sim \text{Normal}\,(\mu = \mu_\alpha,\, \sigma = \sigma_\alpha) \\
\boldsymbol{\beta}_i &\sim \text{Normal}\,(\mu = \mu_\beta,\, \sigma = \sigma_\beta) \\
\boldsymbol{\sigma}_i &\sim \text{Normal}^+\,(\mu = \mu_\sigma,\, \sigma = \sigma_\sigma) \\
\boldsymbol{\tau}_i &\sim \text{Normal}^+\,(\mu = \mu_\tau,\, \sigma = \sigma_\tau) \\
\boldsymbol{m}_{ik} &= \begin{cases} \boldsymbol{\alpha}_i - \frac{1}{2} \cdot \boldsymbol{\beta}_i & \text{if } X_{ik\ell} = 1 \\ \boldsymbol{\alpha}_i + \frac{1}{2} \cdot \boldsymbol{\beta}_i & \text{if } X_{ik\ell} = 2 \end{cases} \\
Y_{ik\ell} &\sim \text{ex-Gaussian}\left(\mu = \boldsymbol{m}_{ik},\, \sigma = \boldsymbol{\sigma}_i,\, \lambda = \tfrac{1}{\boldsymbol{\tau}_i}\right)
\end{aligned}
$$

Ex-Gaussian hierarchial model (λ parameterization)

Figure S5

Ex-Gaussian hierarchical model diagram: λ parameterization

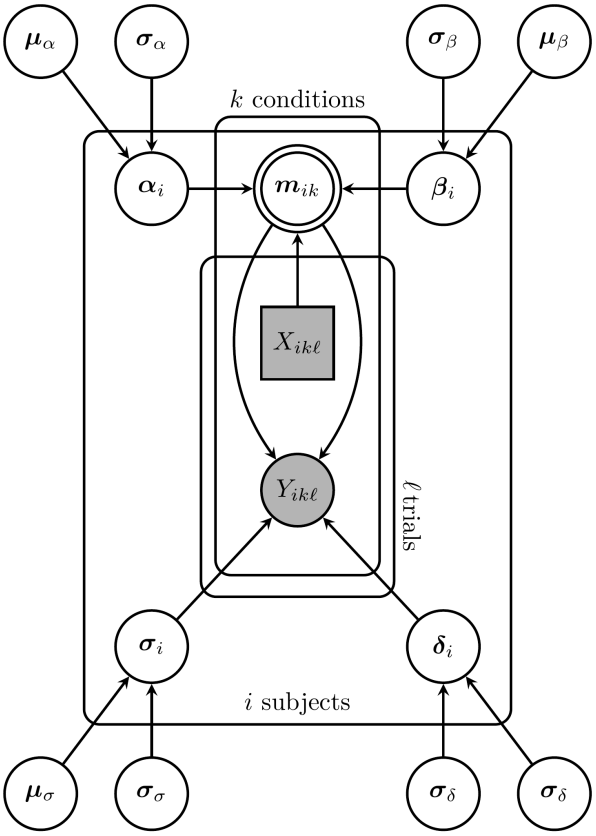


$$
\begin{aligned}
\mu_\alpha &\sim \text{Normal}^+\,(\mu = 0,\, \sigma = 10) \\
\mu_\beta &\sim \text{Normal}\,(\mu = 0,\, \sigma = 10) \\
\mu_\sigma &\sim \text{Normal}^+\,(\mu = 0,\, \sigma = 10) \\
\mu_\lambda &\sim \text{Normal}^+\,(\mu = 0,\, \sigma = 10) \\
\sigma_\alpha &\sim \text{Inverse-Gamma}\,(\alpha = 0.5,\, \beta = 0.5) \\
\sigma_\beta &\sim \text{Inverse-Gamma}\,(\alpha = 0.5,\, \beta = 0.5) \\
\sigma_\sigma &\sim \text{Inverse-Gamma}\,(\alpha = 0.5,\, \beta = 0.5) \\
\sigma_\lambda &\sim \text{Inverse-Gamma}\,(\alpha = 0.5,\, \beta = 0.5) \\
\boldsymbol{\alpha}_i &\sim \text{Normal}\,(\mu = \mu_\alpha,\, \sigma = \sigma_\alpha) \\
\boldsymbol{\beta}_i &\sim \text{Normal}\,(\mu = \mu_\beta,\, \sigma = \sigma_\beta) \\
\boldsymbol{\sigma}_i &\sim \text{Normal}^+\,(\mu = \mu_\sigma,\, \sigma = \sigma_\sigma) \\
\boldsymbol{\lambda}_i &\sim \text{Normal}^+\,(\mu = \mu_\lambda,\, \sigma = \sigma_\lambda) \\
\boldsymbol{m}_{ik} &= \begin{cases} \boldsymbol{\alpha}_i - \frac{1}{2} \cdot \boldsymbol{\beta}_i & \text{if } X_{ik\ell} = 1 \\ \boldsymbol{\alpha}_i + \frac{1}{2} \cdot \boldsymbol{\beta}_i & \text{if } X_{ik\ell} = 2 \end{cases} \\
Y_{ik\ell} &\sim \text{ex-Gaussian}\,(\mu = \boldsymbol{m}_{ik},\, \sigma = \boldsymbol{\sigma}_i,\, \lambda = \boldsymbol{\lambda}_i)
\end{aligned}
$$

Shifted-lognormal hierarchical model

Figure S6

Shifted-lognormal hierarchical model diagram



$$
\begin{aligned}
\mu_\alpha &\sim \text{Normal}^+\,(\mu = 0,\, \sigma = 10) \\
\mu_\beta &\sim \text{Normal}\,(\mu = 0,\, \sigma = 10) \\
\mu_\sigma &\sim \text{Normal}^+\,(\mu = 0,\, \sigma = 10) \\
\mu_\delta &\sim \text{Normal}^+\,(\mu = 0,\, \sigma = 10) \\
\sigma_\alpha &\sim \text{Inverse-Gamma}\,(\alpha = 0.5,\, \beta = 0.5) \\
\sigma_\beta &\sim \text{Inverse-Gamma}\,(\alpha = 0.5,\, \beta = 0.5) \\
\sigma_\sigma &\sim \text{Inverse-Gamma}\,(\alpha = 0.5,\, \beta = 0.5) \\
\sigma_\delta &\sim \text{Inverse-Gamma}\,(\alpha = 0.5,\, \beta = 0.5) \\
\boldsymbol{\alpha}_i &\sim \text{Normal}\,(\mu = \mu_\alpha,\, \sigma = \sigma_\alpha) \\
\boldsymbol{\beta}_i &\sim \text{Normal}\,(\mu = \mu_\beta,\, \sigma = \sigma_\beta) \\
\boldsymbol{\sigma}_i &\sim \text{Normal}^+\,(\mu = \mu_\sigma,\, \sigma = \sigma_\sigma) \\
\boldsymbol{\delta}_i &\sim \text{Normal}^+\,(\mu = \mu_\delta,\, \sigma = \sigma_\delta) \\
\boldsymbol{m}_{ik} &= \begin{cases} \boldsymbol{\alpha}_i - \frac{1}{2} \cdot \boldsymbol{\beta}_i & \text{if } X_{ik\ell} = 1 \\ \boldsymbol{\alpha}_i + \frac{1}{2} \cdot \boldsymbol{\beta}_i & \text{if } X_{ik\ell} = 2 \end{cases} \\
Y_{ik\ell} &\sim \text{Shifted-lognormal}\,(\mu = \boldsymbol{m}_{ik},\, \sigma = \boldsymbol{\sigma}_i,\, \delta = \boldsymbol{\delta}_i)
\end{aligned}
$$

SM7: meta-analysis results

To synthesize the parameter estimates obtained from the Gaussian, Ex-Gaussian, and Shifted-Lognormal multilevel models across the 59 datasets, we conducted a series of multilevel meta-analyses using the `{metafor}` package (Viechtbauer, 2010). For each model parameter (e.g., μ_α, σ_β), the posterior mean estimated from the individual dataset fitting was used as the observed effect size, weighted by the posterior variance as the sampling variance. To ensure distributional assumptions were met and to respect the parameter space, strictly positive parameters (e.g., standard deviations of random effects, σ, τ, shift and scale parameters) were meta-analyzed on the natural logarithmic scale. The resulting pooled estimates and confidence intervals for these parameters were back-transformed (exponentiated) for reporting.

To obtain specific pooled estimates for each experimental paradigm, Task (Flanker, Simon, Stroop) was included as a fixed effect moderator (specified without an intercept). To account for the nested structure of the data – where multiple datasets often originated from the same published study – we included task-specific random effects (i.e., random intercepts for each task type) grouped by study. We specified a diagonal covariance structure, which allows for distinct heterogeneity variances for each task. All models were estimated using Restricted Maximum Likelihood (REML), and standard errors and 95% confidence intervals were computed using the Knapp-Hartung adjustment to ensure robust inference.

Table S2

Meta-analysis Results: Gaussian Model Point Estimates and Confidence Intervals

	Flanker		Simon		Stroop	
Param.	Est.	95% CI	Est.	95% CI	Est.	95% CI
μ_α	0.621	[0.027, 1.215]	0.557	[0.204, 0.910]	0.654	[0.209, 1.099]
μ_β	0.045	[-0.049, 0.139]	0.054	[-0.052, 0.160]	0.064	[-0.009, 0.138]
μ_σ	0.172	[0.106, 0.278]	0.153	[0.085, 0.273]	0.188	[0.113, 0.313]
σ_α	0.098	[0.035, 0.271]	0.086	[0.039, 0.190]	0.115	[0.051, 0.263]
σ_β	0.027	[0.012, 0.062]	0.026	[0.014, 0.047]	0.036	[0.022, 0.059]
σ_σ	0.072	[0.051, 0.102]	0.065	[0.046, 0.093]	0.070	[0.053, 0.093]
shift_σ	0.075	[0.042, 0.133]	0.066	[0.030, 0.145]	0.092	[0.035, 0.239]
scale_σ	0.120	[0.085, 0.169]	0.108	[0.076, 0.155]	0.117	[0.088, 0.155]

Note. Est. represent meta-analitic pooled point estimates.

Table S3

Meta-analysis Results: Ex-Gaussian Model Point Estimates and Confidence Intervals

	Flanker		Simon		Stroop	
Param.	Est.	95% CI	Est.	95% CI	Est.	95% CI
μ_α	0.470	[0.004, 0.937]	0.421	[0.201, 0.640]	0.483	[0.025, 0.942]
μ_β	0.035	[-0.043, 0.112]	0.053	[-0.018, 0.124]	0.038	[-0.041, 0.116]
μ_σ	0.059	[0.023, 0.153]	0.050	[0.029, 0.089]	0.066	[0.034, 0.129]
μ_τ	0.148	[0.077, 0.282]	0.132	[0.070, 0.249]	0.164	[0.084, 0.319]
$\mu_\lambda^\dagger$	7.758	[4.361, 13.802]	8.740	[4.407, 17.334]	6.887	[3.119, 15.208]
σ_α	0.063	[0.017, 0.229]	0.047	[0.021, 0.104]	0.084	[0.024, 0.292]
σ_β	0.021	[0.008, 0.057]	0.023	[0.012, 0.043]	0.025	[0.011, 0.054]
σ_σ	0.021	[0.009, 0.051]	0.015	[0.010, 0.023]	0.025	[0.014, 0.044]
σ_τ	0.004	[0.001, 0.013]	0.004	[0.001, 0.009]	0.004	[0.002, 0.009]
$\sigma_\lambda^\dagger$	14.143	[4.956, 40.356]	17.837	[4.260, 74.689]	8.146	[1.376, 48.221]
shift_σ	0.030	[0.015, 0.059]	0.030	[0.020, 0.045]	0.032	[0.018, 0.058]
shift_τ	0.061	[0.044, 0.085]	0.052	[0.026, 0.103]	0.075	[0.031, 0.178]
$\text{shift}_\lambda^\dagger$	2.847	[1.503, 5.390]	3.063	[1.911, 4.909]	2.840	[1.673, 4.821]
scale_σ	0.035	[0.015, 0.084]	0.026	[0.017, 0.039]	0.041	[0.023, 0.074]
scale_τ	0.106	[0.059, 0.190]	0.100	[0.062, 0.159]	0.108	[0.074, 0.159]
$\text{scale}_\lambda^\dagger$	6.239	[3.693, 10.538]	7.006	[3.424, 14.337]	4.735	[1.946, 11.520]

Note. Est. represents meta-analytic pooled point estimates. † These parameters were estimated using a model with rate (λ) parameterization rather than a τ-based formulation.

Table S4

Meta-analysis Results: Shifted-lognormal Model Point Estimates and Confidence Intervals

	Flanker		Simon		Stroop	
Param.	Est.	95% CI	Est.	95% CI	Est.	95% CI
μ_α	-1.208	[-2.427, 0.011]	-1.288	[-1.943, -0.632]	-1.103	[-1.954, -0.251]
μ_β	0.130	[-0.108, 0.368]	0.217	[-0.214, 0.648]	0.157	[0.001, 0.313]
μ_δ	0.262	[0.061, 0.463]	0.241	[0.185, 0.297]	0.259	[0.110, 0.408]
μ_σ	0.432	[0.332, 0.561]	0.435	[0.359, 0.528]	0.430	[0.306, 0.603]
σ_α	0.273	[0.197, 0.378]	0.238	[0.165, 0.343]	0.275	[0.213, 0.355]
σ_β	0.075	[0.040, 0.139]	0.080	[0.066, 0.096]	0.074	[0.056, 0.098]
σ_δ	0.066	[0.032, 0.138]	0.045	[0.025, 0.081]	0.063	[0.033, 0.124]
σ_σ	0.100	[0.087, 0.115]	0.097	[0.081, 0.117]	0.093	[0.070, 0.124]
shift_σ	0.297	[0.185, 0.476]	0.307	[0.247, 0.381]	0.289	[0.127, 0.660]
scale_σ	0.166	[0.144, 0.190]	0.161	[0.134, 0.194]	0.155	[0.116, 0.206]

Note. Est. represent meta-analitic pooled point estimates.

SM8: population correlation matrices in the simulation study

Unidimensional models

$\boldsymbol{\Lambda} = .3$

$$\mathbf{R}_{\text{uni, .3}} = \begin{bmatrix} 1.000 & 0.090 & 0.090 & 0.090 & 0.090 & 0.090 \\ 0.090 & 1.000 & 0.090 & 0.090 & 0.090 & 0.090 \\ 0.090 & 0.090 & 1.000 & 0.090 & 0.090 & 0.090 \\ 0.090 & 0.090 & 0.090 & 1.000 & 0.090 & 0.090 \\ 0.090 & 0.090 & 0.090 & 0.090 & 1.000 & 0.090 \\ 0.090 & 0.090 & 0.090 & 0.090 & 0.090 & 1.000 \end{bmatrix}$$

$\boldsymbol{\Lambda} = .5$

$$\mathbf{R}_{\text{uni, .5}} = \begin{bmatrix} 1.000 & 0.250 & 0.250 & 0.250 & 0.250 & 0.250 \\ 0.250 & 1.000 & 0.250 & 0.250 & 0.250 & 0.250 \\ 0.250 & 0.250 & 1.000 & 0.250 & 0.250 & 0.250 \\ 0.250 & 0.250 & 0.250 & 1.000 & 0.250 & 0.250 \\ 0.250 & 0.250 & 0.250 & 0.250 & 1.000 & 0.250 \\ 0.250 & 0.250 & 0.250 & 0.250 & 0.250 & 1.000 \end{bmatrix}$$

$\boldsymbol{\Lambda} = .7$

$$\mathbf{R}_{\text{uni, .7}} = \begin{bmatrix} 1.000 & 0.490 & 0.490 & 0.490 & 0.490 & 0.490 \\ 0.490 & 1.000 & 0.490 & 0.490 & 0.490 & 0.490 \\ 0.490 & 0.490 & 1.000 & 0.490 & 0.490 & 0.490 \\ 0.490 & 0.490 & 0.490 & 1.000 & 0.490 & 0.490 \\ 0.490 & 0.490 & 0.490 & 0.490 & 1.000 & 0.490 \\ 0.490 & 0.490 & 0.490 & 0.490 & 0.490 & 1.000 \end{bmatrix}$$

Exploratory Factor Models

$\boldsymbol{\Lambda} = .3$

$$\mathbf{R}_{\text{uni, .3}} = \begin{bmatrix} 1.000 & 0.098 & 0.098 & 0.054 & 0.054 & 0.054 \\ 0.098 & 1.000 & 0.098 & 0.054 & 0.054 & 0.054 \\ 0.098 & 0.098 & 1.000 & 0.054 & 0.054 & 0.054 \\ 0.054 & 0.054 & 0.054 & 1.000 & 0.098 & 0.098 \\ 0.054 & 0.054 & 0.054 & 0.098 & 1.000 & 0.098 \\ 0.054 & 0.054 & 0.054 & 0.098 & 0.098 & 1.000 \end{bmatrix}$$

$\boldsymbol{\Lambda} = .5$

$$\mathbf{R}_{\text{uni, .5}} = \begin{bmatrix} 1.000 & 0.273 & 0.273 & 0.150 & 0.150 & 0.150 \\ 0.273 & 1.000 & 0.273 & 0.150 & 0.150 & 0.150 \\ 0.273 & 0.273 & 1.000 & 0.150 & 0.150 & 0.150 \\ 0.150 & 0.150 & 0.150 & 1.000 & 0.273 & 0.273 \\ 0.150 & 0.150 & 0.150 & 0.273 & 1.000 & 0.273 \\ 0.150 & 0.150 & 0.150 & 0.273 & 0.273 & 1.000 \end{bmatrix}$$

$\boldsymbol{\Lambda} = .7$

$$\mathbf{R}_{\text{uni, .7}} = \begin{bmatrix} 1.000 & 0.534 & 0.534 & 0.294 & 0.294 & 0.294 \\ 0.534 & 1.000 & 0.534 & 0.294 & 0.294 & 0.294 \\ 0.534 & 0.534 & 1.000 & 0.294 & 0.294 & 0.294 \\ 0.294 & 0.294 & 0.294 & 1.000 & 0.534 & 0.534 \\ 0.294 & 0.294 & 0.294 & 0.534 & 1.000 & 0.534 \\ 0.294 & 0.294 & 0.294 & 0.534 & 0.534 & 1.000 \end{bmatrix}$$

Confirmatory Factor Models

$\boldsymbol{\Lambda} = .3$

$$\mathbf{R}_{\text{uni, .3}} = \begin{bmatrix} 1.000 & 0.090 & 0.090 & 0.045 & 0.045 & 0.045 \\ 0.090 & 1.000 & 0.090 & 0.045 & 0.045 & 0.045 \\ 0.090 & 0.090 & 1.000 & 0.045 & 0.045 & 0.045 \\ 0.045 & 0.045 & 0.045 & 1.000 & 0.090 & 0.090 \\ 0.045 & 0.045 & 0.045 & 0.090 & 1.000 & 0.090 \\ 0.045 & 0.045 & 0.045 & 0.090 & 0.090 & 1.000 \end{bmatrix}$$

$\boldsymbol{\Lambda} = .5$

$$\mathbf{R}_{\text{uni, .5}} = \begin{bmatrix} 1.000 & 0.250 & 0.250 & 0.125 & 0.125 & 0.125 \\ 0.250 & 1.000 & 0.250 & 0.125 & 0.125 & 0.125 \\ 0.250 & 0.250 & 1.000 & 0.125 & 0.125 & 0.125 \\ 0.125 & 0.125 & 0.125 & 1.000 & 0.250 & 0.250 \\ 0.125 & 0.125 & 0.125 & 0.250 & 1.000 & 0.250 \\ 0.125 & 0.125 & 0.125 & 0.250 & 0.250 & 1.000 \end{bmatrix}$$

$\boldsymbol{\Lambda} = .7$

$$\mathbf{R}_{\text{uni, .7}} = \begin{bmatrix} 1.000 & 0.490 & 0.490 & 0.245 & 0.245 & 0.245 \\ 0.490 & 1.000 & 0.490 & 0.245 & 0.245 & 0.245 \\ 0.490 & 0.490 & 1.000 & 0.245 & 0.245 & 0.245 \\ 0.245 & 0.245 & 0.245 & 1.000 & 0.490 & 0.490 \\ 0.245 & 0.245 & 0.245 & 0.490 & 1.000 & 0.490 \\ 0.245 & 0.245 & 0.245 & 0.490 & 0.490 & 1.000 \end{bmatrix}$$

SM9: ANOVA meta-models results

Table S5

Effect sizes (ω_p^2) for Correlations and Factor Loadings

	Correlations				Factor loadings				
Predictor	ASRMR	AAB	APSD	AECR	ARMSE	AAB	APSD	AECR	ϕ
DGM	**0.29**	**0.99**	**0.97**	**0.99**	**0.98**	**0.98**	**0.98**	**0.90**	**0.96**
I	**0.99**	**0.91**	**1.00**	**0.99**	**0.98**	**0.97**	**0.99**	**0.92**	**0.98**
L	**1.00**	**1.00**	**0.49**	**1.00**	**0.99**	**0.92**	**1.00**	**0.98**	**1.00**
LF	**0.95**	**0.97**	**0.98**	**0.99**	**0.85**	**0.91**	**0.98**	**0.96**	**0.82**
M	**1.00**	**1.00**	**1.00**	**1.00**	**0.97**	**0.97**	**0.94**	**0.92**	**0.95**
R	**1.00**	**0.99**	**1.00**	**0.99**	**1.00**	**0.99**	**1.00**	**0.82**	**0.99**
DGM x L	**0.90**	**0.97**	0.02	**0.98**	**0.93**	**0.90**	**0.79**	**0.91**	**0.69**
DGM x M	**0.98**	**0.94**	**1.00**	**0.98**	**0.38**	**0.85**	**0.95**	**0.96**	0.00
DGM x R	**0.93**	**0.74**	**0.99**	**0.49**	**0.90**	**0.90**	**0.82**	**0.24**	**0.88**
I x DGM	**0.78**	**0.40**	**0.81**	**0.84**	0.02	0.00	0.05	**0.66**	0.11
I x L	0.00	**0.56**	0.00	**0.96**	**0.63**	**0.37**	**0.71**	**0.75**	**0.94**
I x LF	0.10	**0.17**	**0.69**	**0.46**	**0.58**	**0.61**	**0.79**	**0.52**	**0.45**
I x M	**0.97**	**0.66**	**0.99**	**0.98**	0.00	0.00	0.00	**0.43**	0.00
I x R	**0.92**	**0.72**	**0.99**	**0.67**	0.00	**0.52**	**0.63**	**0.16**	0.08
L x M	**0.98**	**0.99**	**0.53**	**1.00**	**0.85**	**0.83**	**0.69**	**0.90**	**0.79**
LF x DGM	**0.14**	**0.67**	0.00	**0.78**	0.01	**0.14**	**0.34**	**0.68**	0.04
LF x L	**0.75**	**0.90**	**0.71**	**0.97**	**0.95**	**0.98**	**0.97**	**0.91**	**0.95**
LF x M	**0.81**	**0.93**	**0.96**	**0.99**	0.08	0.13	0.09	**0.59**	0.10
LF x R	**0.72**	**0.74**	**0.88**	**0.79**	**0.59**	**0.66**	**0.86**	**0.65**	**0.46**
R x L	**0.97**	**0.98**	**0.56**	**0.98**	**0.94**	**0.87**	**0.91**	0.00	**0.97**
R x M	**0.99**	**0.93**	**1.00**	**0.99**	**0.81**	**0.80**	**0.18**	**0.44**	**0.80**
DGM x L x M	**0.73**	**0.88**	**0.27**	**0.96**	**0.79**	**0.78**	**0.53**	**0.92**	**0.34**
DGM x R x L	0.00	**0.55**	**0.40**	**0.54**	**0.84**	**0.76**	**0.68**	**0.42**	**0.28**
DGM x R x M	**0.98**	**0.85**	**1.00**	**0.93**	0.00	**0.15**	**0.92**	**0.71**	0.00
I x DGM x L	**0.27**	**0.16**	0.11	**0.64**	**0.26**	**0.23**	**0.30**	**0.55**	**0.26**
I x DGM x M	**0.89**	**0.70**	**0.95**	**0.75**	0.10	**0.37**	**0.26**	**0.62**	0.00

Table S5

Effect sizes (ω_p^2) for Correlations and Factor Loadings (continued)

	Correlations				Factor loadings				
Predictor	ASRMR	AAB	APSD	AECR	ARMSE	AAB	APSD	AECR	ϕ
I x DGM x R	**0.75**	0.06	**0.89**	0.00	0.00	0.00	0.00	0.00	0.08
I x L x M	**0.34**	**0.16**	0.00	**0.95**	0.00	0.00	0.02	**0.55**	**0.35**
I x LF x DGM	0.00	0.00	0.00	0.03	0.00	0.00	0.00	**0.39**	0.00
I x LF x L	0.00	0.00	**0.25**	**0.20**	**0.39**	**0.62**	**0.59**	0.13	**0.41**
I x LF x M	0.00	0.00	**0.23**	**0.53**	0.00	0.00	0.00	0.11	0.00
I x LF x R	0.00	0.00	**0.37**	0.03	0.00	0.01	**0.21**	**0.46**	0.08
I x R x L	**0.24**	**0.53**	0.00	**0.79**	**0.52**	**0.44**	**0.54**	0.06	**0.77**
I x R x M	**0.95**	**0.46**	**0.98**	0.09	0.00	0.01	0.00	0.11	0.00
LF x DGM x L	0.01	**0.34**	0.00	**0.67**	0.00	0.04	0.05	**0.77**	0.02
LF x DGM x M	0.04	**0.47**	**0.54**	**0.77**	0.00	0.12	0.00	**0.76**	0.00
LF x DGM x R	0.00	0.00	0.00	0.00	0.00	0.05	**0.15**	0.09	0.04
LF x L x M	**0.76**	**0.83**	**0.38**	**0.97**	0.00	0.00	0.03	**0.73**	**0.22**
LF x R x L	**0.41**	**0.48**	**0.26**	**0.76**	**0.69**	**0.77**	**0.78**	**0.45**	**0.68**
LF x R x M	0.08	**0.45**	**0.55**	**0.56**	0.00	0.02	0.00	**0.17**	**0.16**
R x L x M	**0.81**	**0.83**	**0.50**	**0.96**	**0.59**	**0.54**	**0.43**	**0.30**	**0.23**
DGM x R x L x M	**0.70**	**0.70**	**0.43**	**0.89**	**0.27**	0.09	0.07	**0.41**	0.09
I x DGM x L x M	**0.57**	**0.46**	0.10	**0.79**	0.07	0.04	0.00	**0.46**	0.00
I x DGM x R x L	**0.17**	0.00	**0.17**	**0.21**	0.10	0.00	0.01	0.00	**0.15**
I x DGM x R x M	**0.90**	**0.72**	**0.96**	**0.30**	0.00	**0.24**	0.06	0.02	0.00
I x LF x DGM x L	0.04	0.00	0.00	**0.17**	0.00	0.00	0.00	0.09	0.00
I x LF x DGM x M	0.00	0.00	0.00	0.11	0.00	0.00	0.00	**0.31**	0.00
I x LF x DGM x R	0.00	0.00	0.00	0.00	0.00	0.00	0.00	**0.18**	0.08
I x LF x L x M	**0.18**	0.02	**0.26**	**0.58**	0.00	0.00	0.00	0.11	0.08
I x LF x R x L	**0.23**	0.04	**0.33**	**0.66**	**0.30**	**0.33**	**0.24**	**0.54**	**0.55**
I x LF x R x M	0.00	0.00	0.00	0.09	0.00	0.00	0.00	0.11	0.00
I x R x L x M	**0.17**	**0.14**	**0.21**	**0.85**	0.00	0.00	0.00	0.00	0.05
LF x DGM x L x M	0.10	**0.24**	0.00	**0.61**	0.00	**0.25**	0.09	**0.58**	0.00
LF x DGM x R x L	0.09	0.00	0.00	0.00	0.04	0.00	0.08	**0.14**	**0.18**

Table S5

Effect sizes (ω_p^2) for Correlations and Factor Loadings (continued)

	Correlations				**Factor loadings**				
Predictor	ASRMR	AAB	APSD	AECR	ARMSE	AAB	APSD	AECR	ϕ
LF x DGM x R x M	0.04	0.05	**0.37**	**0.43**	0.00	0.00	0.00	**0.21**	0.00
LF x R x L x M	**0.42**	**0.34**	**0.24**	**0.67**	0.00	0.00	0.00	0.00	0.00
I x DGM x R x L x M	**0.51**	**0.44**	**0.25**	0.00	0.09	0.00	0.00	0.00	0.11
I x LF x DGM x L x M	0.04	0.02	0.08	**0.27**	0.00	0.00	0.00	0.00	0.00
I x LF x DGM x R x M	0.00	0.00	0.00	0.00	0.00	0.00	0.00	0.00	0.00
I x LF x R x L x M	**0.17**	0.00	**0.34**	**0.53**	0.00	0.00	0.00	0.00	0.00
LF x DGM x R x L x M	0.12	0.05	0.00	0.05	0.06	0.12	0.00	**0.31**	0.00

Note. Effect sizes equal or higuer than .14 are marked in bold. I = Sample size (100 or 200). LF = Latent factors (unidimensional, two-factor CFA and two-factor CFA). DGM = Data-Generation Model (ex-Gaussian or Shifted-lognormal). R = Reliability (0.3, 0.5 or 0.7). L = Standardized factor loadings (0.3, 0.5 or 0.7). M = Estimation method (Gaussian HFM or True GenHFM). ASRMR = Average Standardized Root Mean Residuals. AAB = Average Absolute Bias. APSD = Average Posterior Standard Deviation (Average Standard Error in frequentist correlations). AECR = Average Empirical Coverage Rate. ϕ = Tucker Congruence Index.

SM10: Prior distributions used in Viviani et al. reanalysis

Table S6 shows the prior distributios used in the hierarchical component of the exploratory GenHFMs. In all cases, we set uniform priors for all latent factor component parameters (i.e., h^2, $\mathbf{\Lambda}$ and $\mathbf{\Psi}$).

Table S6

Prior distributions used in the Viviani et al. reanalysis for the hierarchical component

Model	Parameter	Prior Distribution
Gaussian	μ_α	Normal($\mu = 0.654, \sigma = 0.453$)
	μ_β	Normal($\mu = 0.064, \sigma = 0.074$)
	shift_σ	Normal$^+$($\mu = 0.092, \sigma = 0.101$)
	σ_α	Student-t^+($\nu = 3, \mu = 0.115, \sigma = 0.105$)
	σ_β	Student-t^+($\nu = 3, \mu = 0.036, \sigma = 0.019$)
	scale_σ	Student-t^+($\nu = 3, \mu = 0.117, \sigma = 0.034$)
Gaussian (iRTs)	μ_α	Normal($\mu = 2.339, \sigma = 1.041$)
	μ_β	Normal($\mu = 0.150, \sigma = 0.172$)
	shift_σ	Normal$^+$($\mu = 0.215, \sigma = 0.239$)
	σ_α	Student-t^+($\nu = 3, \mu = 0.270, \sigma = 0.248$)
	σ_β	Student-t^+($\nu = 3, \mu = 0.083, \sigma = 0.043$)
	scale_σ	Student-t^+($\nu = 3, \mu = 0.273, \sigma = 0.078$)
Ex-Gaussian	μ_α	Normal($\mu = 0.483, \sigma = 0.451$)
	μ_β	Normal($\mu = 0.038, \sigma = 0.079$)
	shift_σ	Normal$^+$($\mu = 0.032, \sigma = 0.021$)
	shift_λ	Normal$^+$($\mu = 2.841, \sigma = 1.570$)
	σ_α	Student-t^+($\nu = 3, \mu = 0.084, \sigma = 0.132$)
	σ_β	Student-t^+($\nu = 3, \mu = 0.025, \sigma = 0.022$)
	scale_σ	Student-t^+($\nu = 3, \mu = 0.041, \sigma = 0.025$)
	scale_λ	Student-t^+($\nu = 3, \mu = 4.735, \sigma = 4.783$)
Shifted-Lognormal	μ_α	Normal($\mu = -1.105, \sigma = 0.862$)
	μ_β	Normal($\mu = 0.157, \sigma = 0.156$)
	μ_δ	Normal$^+$($\mu = 0.259, \sigma = 0.150$)
	shift_σ	Normal$^+$($\mu = 0.289, \sigma = 0.266$)
	σ_α	Student-t^+($\nu = 3, \mu = 0.275, \sigma = 0.071$)
	σ_β	Student-t^+($\nu = 3, \mu = 0.074, \sigma = 0.021$)
	σ_δ	Student-t^+($\nu = 3, \mu = 0.063, \sigma = 0.046$)
	scale_σ	Student-t^+($\nu = 3, \mu = 0.155, \sigma = 0.045$)

Note. Values in parentheses denote location and scale parameters (for Normal) or degrees of freedom, location, and scale (for Student-t). **Gaussian (iRTs):** Priors were obtained by direct transformation of the Gaussian RT priors using the scaling factor $SF = 1/\mu^2_{\alpha,\text{RT}}$, so as to preserve an approximately equivalent degree of prior informativeness under the inverse-RT parameterization. **Ex-Gaussian:** Parameterized using rate (λ) instead of τ, where $\lambda = 1/\tau$. **Notation:** Normal$^+$ and Student-t^+ denote distributions truncated at zero.

SM11: Performance of GenHFMs under a Gaussian Data-Generating Process

Although the main goal of the simulation study was to evaluate the sensitivity of the Gaussian model when data were generated from asymmetric distributions, in this section we addressed the reverse question: how sensitive GenHFMs are when the data-generating process is Gaussian. To do so, we used the meta-parameters of the Gaussian model reported in Table 1 of the main text to generate data from a one-factor model with 100 subjects, varying reliability (.30, .50, and .70) and true factor loadings (.30, .50, and .70). However, the Gaussian model produced some negative observed values, which are incompatible with the nature of RT data and also prevented fitting the shifted-lognormal model. This issue simply reflects a known limitation of the Gaussian model for RTs. To prevent negative values, all simulated RTs were increased by a constant 200 ms, without altering the between-condition differences central to this study.

The results are summarized in Table S7. Overall, the shifted-lognormal GenHFM showed a relatively robust behaviour under this form of model misspecification. Across most fit and recovery indices, its performance was only slightly worse than that of the Gaussian model, and in some cases the differences were negligible. This suggests that the shifted-lognormal model can still recover a broadly similar latent structure even when the data are in fact generated from a Gaussian process. This finding is particularly noteworthy given that, in the main simulation study, fitting a Gaussian model to data generated from a shifted-lognormal process led to much larger discrepancies in parameter estimates. At the same time, however, its convergence diagnostics were clearly less favourable. Although the $\hat{R}$ values remained only moderately elevated, the percentage of divergent transitions was systematically close to 10%, indicating that the sampler encountered persistent difficulties exploring the posterior. In practice, this means that, despite the seemingly acceptable recovery results, interpreting the shifted-lognormal model in this setting would still be risky.

The ex-Gaussian GenHFM behaved substantially worse. Although the Gaussian model is nested within the ex-Gaussian model, estimating a task- and participant-specific τ parameter when its true value is zero appears to create serious difficulties for Hamiltonian Monte Carlo. Fit and

Table S7

Estimated marginal means for fit measures and convergence diagnostics across generating conditions and fitted models under the Gaussian data-generating process

Fit measures: true correlations

		ASRMR			AAB			APSD			AECR		
Factor	Level	G	SL	EG	G	SL	EG	G	SL	EG	G	SL	EG
Reliability	.3	**.12**	.14	.22	**.06**	.09	.25	.17	.16	**.04**	**.97**	.91	.07
Reliability	.5	**.09**	.09	.19	**.04**	.06	.21	.12	.12	**.04**	**.96**	.94	.07
Reliability	.7	**.08**	.08	.17	**.04**	.05	.20	.09	.09	**.03**	**.93**	.92	.07
True $\mathbf{\Lambda}$	.3	.09	.09	**.08**	**.04**	.04	.08	.13	.12	**.03**	.97	**.96**	.16
True $\mathbf{\Lambda}$	.5	**.10**	.11	.18	**.06**	.07	.20	.13	.13	**.03**	**.93**	.90	.04
True $\mathbf{\Lambda}$	.7	**.10**	.11	.32	**.05**	.08	.38	.13	.12	**.04**	**.96**	.91	.00

Fit measures: factor loadings

		ARMSE			AAB			APSD			Tucker's ϕ			AECR		
Factor	Level	G	SL	EG	G	SL	EG	G	SL	EG	G	SL	EG	G	SL	EG
Reliability	.3	**.23**	.26	.46	**.13**	.16	.39	.30	.30	**.13**	**.76**	.74	.35	.99	**.96**	.12
Reliability	.5	**.19**	.20	.37	**.10**	.12	.30	.23	.24	**.10**	**.83**	.80	.58	.98	**.98**	.14
Reliability	.7	**.17**	.18	.32	**.09**	.09	.26	.18	.18	**.09**	**.85**	.85	.68	**.94**	.94	.15
True $\mathbf{\Lambda}$	.3	**.26**	.26	.31	**.18**	.18	.23	.32	.32	**.12**	**.54**	.53	.28	.99	**.99**	.25
True $\mathbf{\Lambda}$	.5	**.21**	.24	.40	**.10**	.13	.34	.25	.25	**.11**	**.92**	.87	.53	.97	**.95**	.12
True $\mathbf{\Lambda}$	.7	**.12**	.14	.44	**.04**	.06	.39	.14	.14	**.09**	**.99**	.98	.80	.96	**.94**	.04

Convergence diagnostics

		$\hat{R}$			Divergences (%)			Max. Treedepth (%)			ESS (%)		
Factor	Level	G	SL	EG	G	SL	EG	G	SL	EG	G	SL	EG
Reliability	.3	**1.01**	1.04	2.30	**.00**	10.49	.00	**.00**	10.64	100.00	**21.06**	13.37	0.13
Reliability	.5	**1.01**	1.04	2.28	**.00**	10.32	.00	**.00**	7.54	100.00	**19.05**	12.83	0.13
Reliability	.7	**1.01**	1.06	2.29	**.00**	11.48	.00	**.00**	11.47	100.00	**16.19**	11.07	0.13
True $\mathbf{\Lambda}$	.3	**1.01**	1.04	2.29	**.00**	9.29	.00	**.00**	11.78	100.00	**18.97**	12.10	0.13
True $\mathbf{\Lambda}$	.5	**1.01**	1.04	2.30	**.00**	10.79	.00	**.00**	7.23	100.00	**17.39**	11.81	0.13
True $\mathbf{\Lambda}$	.7	**1.01**	1.05	2.28	**.00**	12.22	.00	**.00**	10.65	100.00	**19.94**	13.36	0.13

Note. G = Gaussian, SL = shifted-lognormal, and EG = ex-Gaussian. Values are estimated marginal means under the Gaussian data-generating process across the levels of Reliability and True $\mathbf{\Lambda}$. ASRMR = average standardized root mean square residual, ARMSE = average root mean square error, AAB = average absolute bias, APSD = average posterior standard deviation, AECR = average empirical coverage rate, and Tucker's ϕ = coefficient of factor congruence. $\hat{R}$ is the Gelman-Rubin diagnostic. Divergences, Max. Treedepth, and ESS denote the percentages of post-warmup draws with divergent transitions, reaching the maximum treedepth of 10, and contributing to the effective sample size, respectively. Boldface indicates the best-performing fitted model in each row. Lower values are better, except for ESS and Tucker's ϕ; AECR and $\hat{R}$ are preferred when closer to .95 and 1, respectively.

recovery measures were consistently poor, and the convergence diagnostics indicated that the chains failed to mix adequately. In particular, $\hat{R}$ values were far from acceptable, all post-warmup draws reached the maximum treedepth, and the proportion of effective samples was nearly zero. Taken together, these results indicate that the ex-Gaussian model did not function properly under a Gaussian data-generating process.

However, both forms of misspecification also highlighted an important practical advantage: they were accompanied by diagnostic warnings that clearly indicated that the fitted model was not well suited to the data. This stands in contrast to the original simulations in the main text, where the Gaussian model often absorbed asymmetry without producing similarly severe warnings. Here, by contrast, the Stan diagnostics offer applied researchers a useful safeguard: if the data were actually generated by a Gaussian process, the diagnostics would indicate that the shifted-lognormal or ex-Gaussian specification may be inappropriate. It is also worth noting that none of these convergence problems emerged in the empirical illustrations, which further supports the practical adequacy of GenHFMs in applied RT settings, where the assumption of normality is rarely plausible.

SM12: A contamination-mixture extension of the shifted-lognormal GenHFM

As noted in the main text, the shifted-lognormal GenHFM assumes that RTs are generated by a shifted-lognormal model with participant- and task-specific parameters. Although this specification is appropriate when all observed RTs are assumed to arise from the model, it can become problematic in the presence of contaminated responses, such as anticipations, accidental key presses, or lapse-related responses. In such cases, even a small number of implausibly fast observations may pull the shift parameter δ_{ij} toward unrealistically low values, thereby distorting the estimation of the remaining parameters.

To address this issue, we incorporated into our GenHFM framework the contamination-mixture extension of the shifted-lognormal model proposed by Haines et al. (2025). Specifically, we assume that each observed RT may arise from one of two components: a shifted-lognormal component, corresponding to the substantive model of interest, and a contamination component, represented by a uniform distribution[1]. Formally, for participant i, task j, condition k, and trial ℓ, we assume

$$p\left(Y_{ijk\ell}\right) = \begin{cases} \pi_{ij} \cdot f_{\mathcal{U}}\left(Y_{ijk\ell} \mid 0,\, \max\left(Y_{ij\bullet\bullet}\right)\right), & \text{if } Y_{ijk\ell} < \delta_{ij}, \\ \pi_{ij} \cdot f_{\mathcal{U}}\left(Y_{ijk\ell} \mid 0,\, \max\left(Y_{ij\bullet\bullet}\right)\right) + \left(1 - \pi_{ij}\right) \cdot f_{\mathcal{SLN}}\left(Y_{ijk\ell} \mid m_{ijk}, \sigma_{ij}, \delta_{ij}\right), & \text{if } Y_{ijk\ell} \geq \delta_{ij}. \end{cases}$$

Here, $f_{\mathcal{U}}\left(Y_{ijk\ell} \mid 0, \max\left(Y_{ij\bullet\bullet}\right)\right)$ denotes the density of a uniform distribution ranging from 0 to the maximum RT observed for participant i in task j across all conditions and trials, and $f_{\mathcal{SLN}}\left(Y_{ijk\ell} \mid m_{ijk}, \sigma_{ij}, \delta_{ij}\right)$ denotes the density of the shifted-lognormal distribution with location parameter $m_{ijk} = \alpha_{ij} + \beta_{ij} \cdot X_k$, scale parameter σ_{ij}, and shift parameter δ_{ij}. The parameter π_{ij} represents the probability that an RT from participant i in task j arises from the contamination component rather than from the shifted-lognormal component. Under this specification, any observed RT below δ_{ij} is necessarily attributed to the contamination component, because such

[1] Importantly, this extension modifies only the trial-level distributional assumption of the shifted-lognormal GenHFM, while leaving the hierarchical and latent factor structure unchanged. The interpretation of the remaining model parameters therefore remains the same as in the original shifted-lognormal GenHFM.

values fall outside the support of the shifted-lognormal distribution. Thus, the model allows unusually fast observations to be absorbed by the contamination process without forcing the shifted-lognormal component to accommodate them through unrealistically small values of δ_{ij}.

By contrast, RTs greater than or equal to δ_{ij} may still arise either from the contamination component or from the shifted-lognormal component. Still, we expect contamination to remain rare, regardless of whether an RT falls below or above δ_{ij}. Following Haines et al. (2025), we formalized this assumption by assigning π_{ij} a prior centered on a low contamination rate, approximately 5%. Specifically, we modeled the probit-transformed contamination probability as

$$\Phi^{-1}(\pi_{ij}) \sim \mathcal{N}(\mu_{\pi_j}, \sigma_{\pi_j}),$$

with task-specific hyperpriors

$$\mu_{\pi_j} \sim \mathcal{N}(-1.65,\, 0.1), \qquad \sigma_{\pi_j} \sim \text{Student-}t^{+}(4,\, 0,\, 0.5).$$

These priors regularize the model toward low contamination rates unless the data provide clear evidence for a larger contamination component.

We reanalyzed the data from both empirical illustrations using the contamination-mixture extension of the shifted-lognormal GenHFM. Parameter estimates for the shifted-lognormal model and its mixture extension are reported in Tables S8 and S9. In general, the differences between the two models were subtle, and both led to the same substantive inferences about the latent structure. This may be interpreted as evidence that the main conclusions of our reanalyses using the shifted-lognormal GenHFM are fairly robust to contamination processes.

Table S8

Parameter estimates for the shifted-lognormal GHFM and its mixture extension across experiments

Task	Shifted-lognormal						Mixture Shifted-lognormal					
	μ_δ		σ_δ		$\mathbf{\Lambda}$		μ_δ		σ_δ		$\mathbf{\Lambda}$	
	Mean	95% CI	Mean	95% CI	Mean	95% CI	Mean	95% CI	Mean	95% CI	Mean	95% CI
Experiment 1												
Simon	.24	[.23, .24]	.05	[.05, .06]	.19	[.01, .75]	.20	[.19, .21]	.07	[.06, .08]	.21	[.01, .79]
Flanker	.26	[.24, .27]	.09	[.08, .10]	.02	[-.87, .83]	.25	[.23, .26]	.10	[.09, .11]	.07	[-.80, .83]
Stroop	.23	[.22, .24]	.07	[.06, .08]	.11	[-.77, .91]	.23	[.21, .24]	.09	[.08, .10]	.14	[-.75, .88]
Experiment 2												
Simon	.27	[.26, .27]	.05	[.04, .05]	.32	[.01, .91]	.25	[.24, .26]	.04	[.04, .05]	.31	[.01, .91]
Flanker	.29	[.28, .30]	.06	[.05, .06]	.12	[-.66, .82]	.29	[.28, .30]	.05	[.05, .06]	.10	[-.63, .81]
Stroop	.26	[.25, .27]	.04	[.04, .05]	.20	[-.52, .87]	.26	[.26, .27]	.03	[.03, .04]	.17	[-.57, .87]
Experiment 3												
Simon	.26	[.25, .27]	.04	[.04, .05]	.50	[.24, .85]	.24	[.23, .24]	.03	[.03, .04]	.58	[.28, .94]
Flanker	.27	[.27, .28]	.06	[.05, .06]	.38	[.06, .69]	.27	[.26, .28]	.05	[.04, .05]	.36	[.05, .69]
Stroop	.25	[.24, .26]	.04	[.04, .05]	.72	[.36, .98]	.24	[.24, .25]	.04	[.04, .05]	.66	[.33, .97]
All experiments												
Simon	.25	[.25, .26]	.05	[.05, .05]	.60	[.46, .75]	.23	[.22, .24]	.05	[.05, .05]	.64	[.51, .80]
Flanker	.27	[.27, .28]	.07	[.07, .07]	.52	[.37, .66]	.27	[.26, .27]	.07	[.07, .08]	.55	[.40, .68]
Stroop	.25	[.24, .25]	.05	[.05, .06]	.68	[.52, .85]	.24	[.24, .25]	.06	[.05, .06]	.63	[.49, .78]

Note. Mean denotes the posterior mean estimate and CI denotes the 95% credible interval. Rows correspond to tasks, shown separately for each experiment and for the model fitted across all data without distinguishing between experiments. The factor loading for the Simon task was constrained to be positive to identify factor reflection.

Table S9

Parameter estimates for the shifted-lognormal GHFM and its mixture extension

		Shifted-lognormal		Mixture Shifted-lognormal	
Task	Parameter	Mean	95% CI	Mean	95% CI
Peripheral	μ_δ	.27	[.25, .28]	.23	[.20, .25]
	σ_δ	.03	[.01, .05]	.01	[.00, .03]
	λ_1	.92	[.73, .99]	.91	[.72, .99]
	λ_2	.06	[-.14, .27]	.06	[-.14, .26]
Perifoveal	μ_δ	.23	[.22, .25]	.21	[.19, .23]
	σ_δ	.03	[.02, .05]	.02	[.01, .04]
	λ_1	.89	[.68, .99]	.90	[.69, .99]
	λ_2	.01	[-.20, .21]	-.01	[-.22, .19]
Navon	μ_δ	.32	[.31, .34]	.30	[.28, .31]
	σ_δ	.05	[.03, .06]	.03	[.02, .05]
	λ_1	.34	[.00, .68]	.32	[-.02, .67]
	λ_2	.44	[.10, .75]	.42	[.06, .75]
Figure-Ground	μ_δ	.24	[.23, .26]	.17	[.13, .20]
	σ_δ	.03	[.02, .04]	.02	[.00, .03]
	λ_1	-.03	[-.25, .18]	-.05	[-.27, .17]
	λ_2	.94	[.82, 1.00]	.90	[.71, .99]
Flanker	μ_δ	.26	[.25, .28]	.21	[.19, .24]
	σ_δ	.03	[.02, .04]	.02	[.00, .03]
	λ_1	.08	[-.12, .29]	.06	[-.15, .28]
	λ_2	.94	[.82, 1.00]	.90	[.73, .99]
Saliency	μ_δ	.24	[.22, .25]	.21	[.18, .23]
	σ_δ	.03	[.02, .04]	.02	[.01, .03]
	λ_1	.08	[-.23, .39]	.09	[-.22, .43]
	λ_2	.74	[.44, .96]	.71	[.38, .96]

Note. Mean denotes the posterior mean estimate and CI denotes the 95% credible interval. λ_1 and λ_2 denote the standardized factor loadings on Factors 1 and 2, respectively.

References

Anderson, T. W., & Rubin, H. (1956). Statistical inference in factor analysis. In J. Neyman (Ed.), *Proceedings of the third berkeley symposium on mathematical statistics and probability* (Vol. 5, pp. 111–150). University of California Press.

Carvalho, C. M., Chang, J., Lucas, J. E., Nevins, J. R., Wang, Q., & West, M. (2008). High-dimensional sparse factor modeling: Applications in gene expression genomics. *Journal of the American Statistical Association*, *103*(484), 1438–1456. https://doi.org/10.1198/016214508000000869

Greene, W. H. (2011). *Econometric analysis* (7th ed.). Prentice Hall.

Haines, N., Kvam, P. D., Irving, L., Smith, C. T., Beauchaine, T. P., Pitt, M. A., Ahn, W.-Y., & Turner, B. M. (2025). A tutorial on using generative models to advance psychological science: Lessons from the reliability paradox. *Psychological Methods*, 10.1037/met0000674. Advanced Online Publication. https://doi.org/10.1037/met0000674

Mehrvarz, M., & Rouder, J. N. (2025). Estimating correlations in low-reliability settings with constrained hierarchical models. *Behavior Research Methods*, *57*, 59. https://doi.org/10.3758/s13428-024-02568-0

Merkle, E. C., Fitzsimmons, E., Uanhoro, J., & Goodrich, B. (2021). Efficient Bayesian structural equation modeling in Stan. *Journal of Statistical Software*, *100*(6), 1–22. https://doi.org/10.18637/jss.v100.i06

Papastamoulis, P., & Ntzoufras, I. (2022). On the identifiability of bayesian factor analytic models. *Statistics and Computing*, *32*(2), 23. https://doi.org/10.1007/s11222-022-10084-4

Poworoznek, E., Anceschi, N., Ferrari, F., & Dunson, D. B. (2024). Efficiently resolving rotational ambiguity in bayesian matrix sampling with matching. *arXiv Preprint arXiv:2107.13783v2*. https://doi.org/10.48550/arXiv.2107.13783

Rouder, J. N., Kumar, A., & Haaf, J. M. (2023). Why many studies of individual differences with inhibition tasks may not localize correlations. *Psychonomic Bulletin & Review*. https://doi.org/10.3758/s13423-023-02293-3

Viechtbauer, W. (2010). Conducting meta-analyses in R with the metafor package. *Journal of Statistical Software*, *36*(3), 1–48. https://doi.org/10.18637/jss.v036.i03